Geopolitical Mining in Indonesia: Local Environmental and Welfare Costs of the Green Transition

Qiuxia Gao*

March 20, 2026

The clean-energy transition is reshaping the geopolitics of critical minerals, prompting governments to adopt industrial and trade policies aimed at securing battery supply chains. These policies accelerate mining expansion in resource-producing countries, raising concerns about the local environmental and welfare costs of mineral extraction. This paper studies the consequences of nickel mining expansion in Indonesia, the world's largest producer of lateritic nickel and a key supplier to electric-vehicle battery supply chains. Combining administrative mining license records with satellite-based environmental measures and village-level socioeconomic data, I exploit the staggered timing of mine openings between 2012 and 2022 in a difference-in-differences framework. I find that mine openings significantly reduce vegetation cover and increase coastal turbidity, leading to declines in agricultural and fishery output and worsening health outcomes in nearby communities. Exploiting variation in global EV demand growth and Indonesia's 2020 nickel export ban, I further show that geopolitical demand shocks and industrial policies accelerate mining expansion and amplify these local externalities. These results reveal a central tension of the green transition: while its benefits are global, the environmental costs of mineral extraction are concentrated locally and amplified by geopolitical competition.

JEL: Q56, Q34, O13

Keywords: Green transition, Geopolitical mining, Environmental externalities, Global South

*Department of Real Estate, National University of Singapore; Email: e0610864@u.nus.edu

1 Introduction

The global transition toward clean energy is reshaping not only energy systems but also the geopolitics of natural resources. As demand for critical minerals rises rapidly, major economies—including the United States, the European Union, and China—have adopted industrial policies aimed at "de-risking" supply chains, reducing dependence on geopolitical rivals, and securing access to upstream mineral resources (Zamanillo and Rivera, 2025; Overland, 2019). This intensifying competition places resource-producing countries at the center of global supply chain strategy, creating strong incentives for their governments to intervene in resource markets and capture greater value from extraction. One prominent policy response is the growing use of export restrictions including tariffs, quotas, and export bans—to regulate mineral supply and encourage domestic processing. Figure 1 shows a strong positive relationship between geopolitical risk and the use of trade policy interventions, particularly export-related measures. These patterns suggest that resource countries increasingly deploy export restrictions as strategic tools in response to geopolitical uncertainty (Nygaard, 2022; Udeaja et al., 2024).

[Insert Figure 1 here]

Such policies accelerate domestic mining development, expanding extraction and concentrating environmental pressures in the rural and coastal communities where mining takes place. Yet these local costs are largely overlooked in existing discussions of the clean-energy transition, which tend to focus on aggregate decarbonization outcomes while ignoring the upstream environmental and welfare consequences borne by mineral-producing regions. Moreover, these policies aimed at securing mineral supply often attract substantial foreign direct investment into processing sectors. Whether such investment leads to cleaner production through technology transfer and stronger environmental standards, or instead intensifies environmental pressures through rapid extraction, remains an open empirical question.

To fill this gap, this paper examines the local environmental and socioeconomic consequences of mining expansion during the clean-energy transition. Nickel provides a particularly useful setting. As a key input for lithium-ion batteries, global nickel demand is projected to increase several-fold by 2040, driven by the rapid adoption of electric vehicles[1] (Gielen, 2021). Indonesia holds the world's largest nickel reserves and has emerged as the

[1] See Carbon Credits.

dominant global producer (Figure A1), placing the country at the center of strategic competition over battery supply chains. Nickel mine openings in Indonesia are dispersed across time and geography, generating variation in the timing and location of mining entry that allows me to estimate how mining expansion affects nearby communities. At the same time, Indonesia has adopted industrial policies aimed at capturing more value from its mineral resources. In response to rising global demand, the government implemented a nationwide export ban on raw nickel ore in 2020 to promote domestic processing. Following the policy, both the number and spatial footprint of nickel mines increased markedly (Figure 2), reflecting a rapid expansion of mining activity across many rural and coastal districts. The 2020 export ban therefore provides a policy shock that allows me to examine whether geopolitical forces amplify the local consequences of mining activity.

[Insert Figure 2 here]

Specifically, I implement a spatial difference-in-differences design that compares communities within 30 kilometers of new mine openings to nearby unexposed areas before and after entry. To examine the role of geopolitical forces, I further exploit variation in global EV demand and Indonesia's 2020 export ban in a triple-difference framework to test whether geopolitical shocks amplify the local externalities of mining expansion. The analysis combines administrative data on mining licenses with high-resolution satellite measures of vegetation cover and water quality, as well as village-level socioeconomic surveys. The results show that mine openings lead to significant environmental degradation. Vegetation cover (NDVI) declines by approximately 2 percent near new mines, while coastal water turbidity (KD490) increases by about 2.5 percent, indicating deterioration of both terrestrial and marine ecosystems. These environmental shocks translate into economically meaningful consequences for nearby communities. Agricultural production falls by roughly 12 percent in exposed areas, fishing activity declines in coastal communities, and water-borne illnesses increase. Importantly, local labor markets do not fully offset these losses through mining-related employment gains.

Geopolitical forces further amplify these effects. Indonesia's 2020 nickel export ban significantly increased domestic mining activity and magnified environmental degradation near affected sites. Similarly, periods of rapid growth in global electric vehicle demand are associated with greater mining expansion and larger local environmental losses. More broadly, these findings highlight a central tension of the green transition: while the environmental benefits of clean technologies accrue globally, the environmental costs of mineral extraction are

concentrated locally and disproportionately borne by vulnerable rural communities. These costs are further amplified by geopolitical competition that accelerate resource extraction.

This paper makes three contributions. First, this paper shows that geopolitically motivated industrial and trade policies used to secure critical minerals can impose substantial environmental and welfare costs on resource-producing countries. Existing work largely focuses on strategic competition among major powers, trade policy design, and national industrial strategies (Farrell and Newman, 2019; Baldwin and Freeman, 2022; Overland, 2019), but provides limited evidence on how geopolitically driven mineral expansion affects local communities in producing countries. Exploiting variation in global EV demand and Indonesia's 2020 nickel export ban in a triple-difference framework, this paper shows that geopolitical forces significantly accelerate mining expansion and amplify local environmental and socioeconomic costs. The findings provide new micro-level evidence that strategic competition over critical minerals systematically reallocates environmental burdens toward resource-producing regions in the Global South. They further suggest that these costs are not simply a byproduct of comparative advantage, but arise from deliberate industrial and geopolitical strategies, highlighting the importance of international governance in addressing upstream environmental externalities.

Second, this paper reveals that policies driving the clean-energy transition generate significant upstream environmental and welfare costs that are largely overlooked in current policy evaluation. Prior work documents that environmental policies in high-income countries can generate "North–South displacement effects" by relocating pollution-intensive activities to developing economies (Copeland, 2000; Levinson and Taylor, 2008; Tanaka et al., 2022). Similarly, the process of decarbonization can generate localized environmental damage and social disruption in regions with weaker governance (GONZÁLEZ-ESPINOSA et al., 2025; Besley and Persson, 2023; Llamas-Orozco et al., 2023; Shen et al., 2024). However, how these dynamics operate through upstream mineral extraction—the critical input for clean technologies—remains poorly understood (Peñaloza-Pacheco et al., 2025). This paper fills that gap by showing how growth in global EV demand propagates through supply chains to expand mining activity and generate local environmental and welfare costs in mineral-producing regions. The results demonstrate that the North–South displacement of environmental burdens extends beyond the relocation of polluting industries to include upstream extraction within ostensibly clean supply chains.

Third, this paper demonstrates that conventional policy evaluations substantially underestimate the welfare costs of mineral extraction by failing to account for environmental transmission channels. It provides unified causal evidence on the joint environmental and

welfare consequences of large-scale mineral expansion. Prior research has examined either the environmental impacts of mining—such as deforestation, ecosystem degradation, and pollution—or its economic consequences for labor markets and local development (Aragón and Rud, 2013, 2016; Von der Goltz and Barnwal, 2019; Michaels, 2011; Allcott and Keniston, 2018; Xie et al., 2025). Even studies using quasi-experimental methods typically focus on a single margin, and few trace how environmental degradation—particularly in coastal and marine ecosystems—translates into welfare losses for communities dependent on agriculture and fisheries. This paper addresses that gap by exploiting the staggered timing and geographic distribution of nickel mine openings in Indonesia to jointly identify impacts on both terrestrial and marine ecosystems and their downstream effects on agriculture, fisheries, and health. The results show that the welfare costs of extraction operate substantially through ecosystem degradation rather than labor market channels alone, implying that analyses focusing solely on income or employment substantially understate the true burden of mining on rural communities.

The remainder of this paper is structured as follows. Section 2 outlines the background information. Section 3 illustrates our data and identification strategy. Section 4 presents our empirical findings on the local impacts of nickel mining. Section 5 delves into the discussion of the intensification of geopolitical drivers. Section 6 concludes

2 Background Information

2.1 Global Nickel Demand and Supply

Nickel is a highly versatile metal with long-standing applications across a range of industries. Historically, it has been a key input in stainless steel production, enhancing strength and corrosion resistance, as well as in specialized alloys used in aerospace and heavy industry. More recently, however, nickel's most rapidly expanding and strategically important application has emerged in lithium-ion batteries, which are central to the global clean-energy transition—particularly the electrification of transportation (Lo et al., 2024; Ou et al., 2019). A typical 62.5 kWh EV battery contains approximately 43 kg of nickel, making it one of the largest and most cost-intensive material inputs in lithium-ion battery production.[2] As major markets—including China, the United States, and Europe—adopt increasingly ambitious EV deployment targets, battery manufacturing has become the dominant driver of global

[2]For more details, see Carbon Credits.

nickel demand. This trend is further reinforced by the electronics sector, with manufacturing hubs such as South Korea relying heavily on nickel for electronic components. Hence, rising demand from electric mobility and electronics has transformed nickel from a traditional industrial metal into a strategic resource that is central to the global decarbonization agenda.

On the supply side, Indonesia plays a pivotal role in meeting this surge in demand due to its vast endowment of high-quality laterite nickel ore. While nickel is produced in multiple regions worldwide, Indonesia holds the world's largest laterite reserves—the primary feedstock for producing Class-1 nickel required for EV batteries (Specker et al., 2024). These reserves are economically scalable using established processing technologies such as High Pressure Acid Leach (HPAL) and Rotary Kiln Electric Furnace (RKEF), which enable the production of battery-relevant intermediates, including mixed hydroxide precipitate (MHP) and nickel matte. In contrast, major producers such as Canada and Australia in Figure A1 rely predominantly on sulfide deposits, which face declining ore grades, higher extraction costs, and increasing operational challenges due to remoteness. Other laterite-producing countries, including the Philippines and New Caledonia, also contribute to global supply but are constrained by smaller or more fragmented reserves, as well as environmental and political restrictions. As a result, supply expansion outside Indonesia has remained limited, heightening Indonesia's strategic importance in global battery-grade nickel markets.

Indonesia's role is further reinforced by the geographic concentration of its laterite deposits in coastal regions shown in the Figure A2, such as Sulawesi and Kalimantan, which facilitates large-scale open-pit mining and reduces transportation costs for both raw ore and processed materials. Overall, Indonesia's resource endowment, processing capacity, and geographic advantages position it as a central node in the global nickel supply chain underpinning the clean-energy transition. At the same time, this concentration of production raises critical questions about how rising global demand for "clean" technologies reshapes local environments, economies, and welfare in resource-producing regions.

2.2 Indonesia's Nickel Export and Industrial Policy

Indonesia's push for domestic value-added processing in the mining sector reflects a long-term strategy of resource-based industrialization aimed at increasing the economic value captured from its abundant mineral endowments and strengthening its position in global value chains. This downstreaming agenda—locally referred to as *hilirisasi* unfolded gradually over the past decade, reshaping incentives for extraction, processing, and foreign investment over

time. The institutional foundation of this strategy was laid by the *Mineral and Coal Mining Law*, which articulated the government's intention to restrict exports of unprocessed mineral ores and promote domestic smelting and refining. Beginning in the early 2010s, this framework generated evolving policy signals and expectations among mining firms. An initial export ban on unprocessed nickel ore was introduced in 2014, but its effectiveness was weakened by limited domestic processing capacity, uneven enforcement, and the widespread use of exemptions. Between 2017 and 2019, the government temporarily relaxed restrictions through quota-based export arrangements, reflecting an attempt to balance downstream ambitions with short-run constraints faced by the mining sector. In January 2020, the government fully reinstated the export ban on unprocessed nickel ore with substantially stricter enforcement. Unlike earlier policy prohibition, the 2020 ban eliminated most exemptions and effectively required mining firms to invest in domestic processing or foreign investment (Lahadalia et al., 2024; Ramadhani and Paksi, 2025a).

Over the broader 2012–2022 period, these evolving policy signals progressively reshaped investment incentives along the global nickel supply chain. Mining firms faced growing pressure to integrate downstream, while Indonesia's abundant laterite endowment—combined with its industrial policy direction—attracted substantial foreign direct investment, particularly from Chinese and South Korean firms, into smelting, refining, and precursor-processing activities. This surge in investment drove the rapid emergence of large, spatially concentrated industrial zones such as the Morowali Industrial Park in Central Sulawesi and the Weda Bay Industrial Park in North Maluku, which integrate mining, smelting, and processing within tightly clustered locations (Ramadhani and Paksi, 2025b). To illustrate these structural changes, I use annual bilateral commodity-level trade data from CEPII. Figure 3 shows a pronounced shift in Indonesia's nickel export composition since the mid-2010s, characterized by a collapse in raw nickel ore exports and a rapid expansion of processed intermediates. The right panel further indicates that these intermediate exports are highly concentrated among a small number of importing countries, led by South Korea and China, highlighting Indonesia as a key upstream node in global battery and industrial supply chains.

[Insert Figure 3 here]

While downstreaming succeeded in increasing nickel-related investment and domestic processing capacity, it did not fundamentally alter Indonesia's position within the higher-value segments of global production networks. Advanced downstream activities—such as cathode material production, battery-cell manufacturing, and EV assembly—remain largely concentrated in China, South Korea, and advanced economies, leaving Indonesia primarily

specialized in energy-intensive, pollution-intensive midstream processing. Ownership and control over technology, pricing, and market access are similarly dominated by foreign firms, raising concerns that downstreaming has generated a form of refined dependence: industrial upgrading in form, but continued externalization of high-value functions and decision-making power (Ramadhani and Paksi, 2025b). Moreover, much of the nickel extraction and downstreaming industrial expansion occurred in rural, coastal, and forested areas such as Sulawesi, North Maluku. Reports of deforestation, water pollution, coastal sedimentation, and social conflict have intensified in these regions, while environmental enforcement capacity has struggled to keep pace with the speed of industrial growth[3]. As a result, while the economic benefits of downstreaming are distributed globally through clean-energy supply chains, many of the environmental and social costs remain localized within Indonesia (Astuti et al., 2025).

I focus on the 2012–2022 sample period to capture the full arc of Indonesia's nickel downstreaming process—from early mine openings and gradual policy tightening to large-scale industrial clustering and deeper integration into global clean-energy supply chains. This longer horizon provides rich variation in the timing and location of mine openings and downstream investments, enabling an analysis of sustained expansion in nickel extraction. By moving beyond a narrow evaluation of a single export ban, the paper examines the cumulative local consequences of a decade-long transformation of Indonesia's nickel sector under the global green transition.

2.3 Environmental Governance in Indonesia

The environmental consequences of Indonesia's mining boom are shaped not only by the scale of extraction but also by weaknesses in the country's regulatory and institutional framework. Indonesia has established a comprehensive set of environmental and land-use regulations intended to mitigate the ecological impacts of mining, including the *Forestry Law, Land Conversion Rules*, and *Mandatory Environmental Impact Assessments* (AMDAL). In principle, mining companies are restricted from clearing primary forests without special permits, must obtain formal approval before converting agricultural land, and are required to manage tailings and wastewater in accordance with standards set by the Ministry of Environment and Forestry. In practice, however, compliance with these regulations has been uneven, with substantial variation in enforcement across regions.

[3]See, for example, Eco-Business and Mongabay.

A key source of regulatory enforcement gaps in Indonesia stems from decentralization reforms initiated in the early 2000s, which transferred substantial authority over land allocation, mining permits, and environmental approvals to district and provincial governments. While decentralization aimed to improve administrative efficiency and promote local development, it also created incentives for local governments to prioritize short-term fiscal and political gains over environmental protection. As documented by Burgess et al. (2012), similar political incentives accelerated deforestation through rent-seeking land allocations. Comparable dynamics operate in the mining sector, where local governments benefit from issuing extraction licenses, often approving projects in ecologically sensitive or agriculturally productive areas. As a result, formal safeguards such as Environmental Impact Assessments (AMDAL) are frequently treated as procedural requirements rather than binding constraints, and monitoring and enforcement of land-use and water-quality regulations remain weak. These institutional limitations are particularly pronounced in nickel-producing regions, where rapid mining and smelter expansion—driven by downstreaming policies and foreign investment—has outpaced the capacity of regulatory institutions to manage associated environmental risks.

3 Data and Empirical Strategy

3.1 Data Sources

Mining data: I obtain detailed information on mining activities from Indonesia's Ministry of Energy and Mineral Resources (MEMR), which provides a comprehensive dataset on licensed mining permits and mining sites nationwide. For each site, the database reports key attributes, including mineral type, geographic coordinates, estimated reserves, start year, and operational status (e.g., exploration, active, closed, or under development). This dataset allows me to identify both nickel and non-metal mines, which I use to conduct placebo tests in the robustness check. The precise geographic coordinates of each mine form the basis for linking environmental outcomes to mining activity and for calculating distances used to estimate localized effects. I restrict the sample to mines classified as operational from 2012-2022, ensuring that the analysis captures environmental impacts associated with active nickel extraction.

Vegetation cover data: To quantify changes in vegetation cover near mining areas, I use NASA's MODIS Normalized Difference Vegetation Index (NDVI), which provides

monthly observations at a 1 km spatial resolution. NDVI is derived from near-infrared and red reflectance and is widely used as an indicator of vegetation density and ecosystem health in studies of deforestation and land-use change. In the analysis, each NDVI grid cell is matched to the nearest mining site to capture localized vegetation responses associated with mining operations, land clearing, and smelter construction. The dataset spans the period from 2012 to 2022, allowing me to examine both short- and medium-run changes in vegetation cover following nickel mine openings.

Ocean turbidity data: To assess water-quality impacts in coastal mining regions, I use the KD490 index from NASA's COPE OceanColor product over the 2012–2022 period. This dataset provides monthly global coverage at a 4 km spatial resolution and is widely used to monitor coastal water conditions. KD490 represents the diffuse attenuation coefficient at a wavelength of 490 nm and captures the extent to which light is absorbed or scattered by particulate matter in seawater. Higher KD490 values indicate greater turbidity and reduced water clarity, reflecting increased sediment loads, plankton concentration, or other suspended particulates. KD490 is therefore a standard proxy for tracking sediment plumes and coastal turbidity associated with mining-related erosion and runoff. I then link KD490 grid cells to nearby nickel mining sites and define treatment and control areas based on distance to mine locations in main analysis.

Agricultural production data: Agricultural production is measured using the Global Gridded Crop Production dataset (GGCP10) developed by Qin et al. (2023) and available through the Harvard Dataverse. GGCP10 provides annual, spatially explicit estimates of crop production at a 10 km $\times$ 10 km resolution for the period 2012–2020, covering four major staple crops: maize, wheat, rice, and soybean. For each crop–year, grid-cell values report total production in kilotons. The high spatial resolution and consistent temporal coverage make GGCP10 well suited for analyzing localized agricultural responses to environmental disturbances. I use grid-level crop production as the outcome variable and similarly link each grid cell to the nearest nickel mine. The analysis focuses on crop categories that are most representative of rural agricultural production in Indonesia, including maize, rice and soybean.

Fishing ship data: Fishing activity is measured using data from Global Fishing Watch (GFW), which provides spatially explicit information on fishing effort and vessel movements derived primarily from Automatic Identification System (AIS) signals. GFW combines satellite-based vessel tracking with machine-learning algorithms to classify fishing behavior at high spatial and temporal resolution. I use monthly gridded measures of fishing effort and fishing vessel density at a 10 km $\times$ 10 km resolution to proxy local fisheries activity.

Fishing effort is measured as hours of active fishing within each grid cell, while vessel density captures the number of fishing vessels observed over time. These measures allow me to quantify changes in fisheries activity in coastal waters potentially affected by mining-induced marine pollution.

In addition, I use AIS-based vessel density data from GFW to proxy port activity and maritime traffic intensity. Because port throughput and industrial shipping are closely linked to vessel presence near coastal infrastructure, vessel density provides a consistent, high-frequency indicator of port-related economic activity, particularly in regions where administrative port statistics are unavailable or incomplete. The high spatial resolution and global coverage of GFW data make them particularly suitable for capturing localized and heterogeneous marine responses to coastal industrial expansion. Grid-level fishing effort and vessel density are spatially linked to the nearest nickel mine based on geographic distance, enabling consistent treatment–control comparisons across marine outcomes.

Village Socioeconomic Data: Socioeconomic outcomes are measured using the Village Potential Survey (PODES), conducted by Indonesia's Central Bureau of Statistics. The survey covers all administrative villages nationwide and is collected approximately every three years, providing comprehensive information on local economic activities, public infrastructure, environmental conditions, and reported sources of pollution. For this analysis, I use the 2018 and 2021 waves of PODES, which bracket the period of rapid nickel mining expansion and downstream industrial development. The near-complete coverage of all administrative villages ensures that both mining-affected and non-affected areas are well represented, supporting a credible assessment of the socioeconomic consequences of mining expansion. After using village names to merge village geographical locations, I then spatially match each village to nearby nickel mining sites and apply the same treatment definition as in the environmental analysis. The census-like scale of PODES enhances representativeness and enables systematic comparisons across villages experiencing different degrees of exposure to mining activity.

Control variables: Because ocean currents influence sediment dispersion, I include controls derived from the Copernicus Marine Environment Monitoring Service (CMEMS). The CMEMS reanalysis provides monthly global oceanographic variables at a 0.083° resolution, including current speed and direction, sea surface temperature, and mixed-layer thickness. These variables are bilinearly interpolated onto the KD490 grid and serve as essential controls to account for natural variation in ocean mixing and circulation that could otherwise confound the observed effects of mining on turbidity. To account for weather-related patterns that influence vegetation and water quality, I incorporate meteorological data from

NOAA. The dataset includes monthly measures of temperature, wind speed, precipitation, and dew point, collected at the monitor level. I match these variables to the analysis grids using an inverse-distance weighting scheme. These controls help net out climatic variation that may independently affect forest greenness or sediment runoff.

3.2 Identification Strategy

To estimate the causal effects of nickel mine openings on local environmental conditions, I implement a difference-in-differences (DiD) design that compares grid cells located within 30 km of nickel mines with control grid cells before and after the issuance of mining extraction permits. The empirical specification is as follows:

$$Ln(Y_{imt}) = \beta_0 + \beta_1 Treat_{im} * Post_t + \eta X_{it} + \delta_i + \zeta_m + \tau_t + \gamma_{rt} + \epsilon_{imt} \tag{1}$$

The dependent variable Y_{imt} measures environmental and socioeconomic outcomes for grid cell or village i located near nickel mine site m in year–month t. Depending on the specification, outcomes include monthly vegetation conditions (NDVI), ocean turbidity (KD490), agricultural production, fishing effort, or village-level socioeconomic indicators. The treatment indicator $Treat_{im}$ equals one if grid cell or village i lies within 30 kilometers of its nearest nickel mine, and zero if it is located between 30 and 50 kilometers from the nearest mining site. We adopt the 30-kilometer cutoff based on two considerations. First, prior studies document that the environmental impacts of mining—such as deforestation and marine pollution—are highly localized and concentrated within comparable spatial ranges (Aragón and Rud, 2016). Second, distance-band analyses show that estimated effects are largest and statistically significant within 30 kilometers of mine sites and attenuate rapidly beyond this radius. The indicator $Post_t$ equals one for periods after the start of mining operations at site m. The vector X_{it} includes time-varying environmental controls that may independently affect terrestrial and marine outcomes, including ocean current direction and speed, sea surface temperature, mixed-layer depth, precipitation, wind speed, ambient temperature, and dew point. These covariates flexibly account for natural climatic and oceanographic variation.

All specifications include a rich set of fixed effects. Grid fixed effects δ_i absorb time-invariant unobserved heterogeneity at the grid-cell level. Mine-site fixed effects ζ_m control for baseline differences across mine locations, such as geography and pre-existing ecological conditions. Year–month fixed effects τ_t capture common shocks, including seasonality and national macroeconomic trends. In addition, province-by-year fixed effects γ_{rt} flexibly control

for time-varying regulatory environments and province-specific trends. Standard errors are clustered at the grid level. Because locations closer to mine sites are more directly exposed to land clearing, sediment runoff, and industrial activity, observations are weighted by the inverse of their distance to the nearest mine. This weighting scheme assigns greater influence to locations experiencing higher treatment intensity while preserving the spatial structure of exposure.

Given the environmental footprint of open-pit mining and associated land clearing and sediment runoff, we expect mining expansion to reduce local vegetation cover, implying a negative treatment effect on NDVI. For marine outcomes, increased sedimentation and coastal disturbance are expected to worsen nearshore water quality, implying a positive treatment effect on KD490 (higher turbidity). We further expect declines in agricultural production in exposed areas due to soil degradation and reduced land productivity. Predictions for fishing effort are potentially ambiguous: environmental degradation may reduce the profitability of fishing and lower activity, but it may also induce compensatory increases in effort if vessels must travel farther or fish longer to maintain catches. Finally, for village-level outcomes, we expect patterns consistent with worsening environmental conditions and livelihood disruption, including deteriorations in health-related indicators and shifts in local economic activity away from agriculture and fisheries.

4 Local Environmental and Economic Inequality from Nickel Mine

4.1 Impacts on Environment: Forest and Ocean

Figure 4 documents a clear spatial decay in the environmental impacts of mine openings and provides direct evidence supporting our choice of a 30-kilometer treatment boundary. I estimate separate effects for 5-kilometer rings around each mine and find that both vegetation cover and ocean turbidity exhibit large and statistically meaningful responses only within close proximity to the mine site. NDVI declines by roughly 2–3 percentage points within the first 10–15 km, while KD490 increases sharply—peaking at 0–5 km and diminishing steadily through the 15–20 km band. Beyond 25–30 km, the point estimates for both outcomes converge tightly toward zero and remain statistically indistinguishable from zero across all distance bands. This sharp attenuation indicates that the environmental externalities of nickel extraction are highly localized and do not propagate beyond a 30-kilometer radius.

Accordingly, defining treated areas as locations within 30 km of a mine captures the full extent of the mine-related environmental footprint while ensuring that locations beyond this threshold are valid untreated controls.

[Insert Figure 4 here]

Baseline results: Building on the graphical evidence in Figure 4, I employ difference-in-differences models comparing environmental outcomes in treated grids within 30 km of nickel mines to control grids farther away, before and after mine openings. Table 1 reports the baseline estimates for terrestrial vegetation (Panel A) and coastal water quality (Panel B). Column (1) presents results from the most parsimonious specification, which controls for climatic variables as well as grid-cell and year-month fixed effects. Consistent with the spatial patterns shown in Figure 4, monthly NDVI declines by approximately 1.8 percent in areas exposed to nickel mining, while ocean color KD490 increases by about 2.2 percent, both statistically significant. To mitigate concerns about unobserved confounders at finer geographic and administrative levels, Columns (2) and (3) sequentially add mine fixed effects and province-by-year fixed effects. The estimated coefficients remain highly stable in both magnitude and significance, indicating that the results are not driven by time-invariant mine characteristics or province-specific shocks. In Column (4), I further restrict the control group to grids located 30–50 km from mine sites, addressing the possibility that other confounders beyond more distant control areas. Under this more conservative comparison, NDVI declines by about 2.0 percent and KD490 increases by roughly 2.5 percent. This specification serves as the preferred baseline, as it absorbs time-invariant unobservables at the grid level while also controlling for time-varying regional shocks.

To interpret the economic and ecological significance of these magnitudes, I draw on existing literature. In humid tropical regions, a 2–3 percent decline in NDVI corresponds to an estimated 6–8 percent reduction in forest cover, a magnitude commonly associated with substantial anthropogenic forest degradation and meaningful losses in carbon stocks and climate resilience (Gutman and Ignatov, 1998; Hansen et al., 2013); see also Our World in Data. For marine environments, remote-sensing studies document that a 5–10 percent increase in KD490 in nearshore waters is typically associated with a 15–30 percent rise in turbidity and suspended particulate matter. In coastal and nearshore systems, such changes are widely interpreted as material deterioration in water quality (Binding et al., 2010). Moreover, KD490 enters the underwater light field through an exponential attenuation process (Kirk, 1994), implying that even a 2–3 percent increase in KD490 can translate into a 5–10 percent reduction in light availability at typical coastal depths, with direct consequences

for primary production (Cloern, 2001). Hence, the baseline estimates imply substantial degradation of both terrestrial and marine ecosystems following nickel mine openings.

[Insert Table 1 here]

Robustness check: Table 2 presents a series of robustness checks designed to address key identification concerns. Column (1) reproduces the preferred baseline estimates. Column (2) trims the top and bottom 1 percent of NDVI and KD490 observations to ensure that the results are not driven by extreme outliers or measurement error. Column (3) implements a placebo test by assigning treatment to non-metal mine openings, which are unlikely to be affected by nickel-specific supply-chain dynamics. Column (4) adopts heteroskedasticity- and autocorrelation-consistent (HAC) spatial standard errors to account for serial correlation and spatial dependence. Because two-way fixed-effects DiD estimators may be biased under staggered treatment timing and heterogeneous treatment effects, Column (5) reports estimates using the CSDID approach. Across all specifications, the results remain remarkably stable. In Panel A, the estimated treatment effects on vegetation range from –0.014 to –0.020, implying a roughly 2 percent decline in NDVI within 30 km of mine sites following mine openings. Panel B shows similarly robust effects on coastal water quality, with KD490 increasing by approximately 2.5–3 percent across specifications, consistent with heightened sediment dispersion and marine pollution. Importantly, the placebo estimates in Column (3) are small and statistically insignificant in both panels, providing reassurance that the baseline findings are not driven by pre-existing trends or correlated local development patterns. Overall, the robustness checks confirm that the observed declines in vegetation and deterioration in coastal water quality reflect causal environmental impacts of nickel mining expansion rather than modeling choices or spurious correlations.

[Insert Table 2 here]

Overall, nickel mining activity leads to substantial deforestation and coastal sedimentation in surrounding areas. To further assess the validity of the difference-in-differences design, Figure 5 presents an event-study analysis that traces the dynamic responses of vegetation cover and ocean turbidity around the timing of mine openings. The event-study estimates show no evidence of differential pretrends. In the years preceding mine openings, the coefficients are small, fluctuate around zero, and are statistically indistinguishable from zero for both NDVI and KD490. This pattern indicates that treated and control areas followed common environmental trends prior to treatment, lending support to the parallel-trends

assumption underlying the DID framework. In contrast, immediately after mine openings (year 0), both outcomes display sharp and persistent divergences. NDVI declines markedly, while KD490 rises, consistent with large-scale land clearing and increased sediment runoff associated with mining activity. These dynamic patterns reinforce the baseline results and strengthen the credibility of the identification strategy.

[Insert Figure 5 here]

4.2 Impacts on Rural Production: Agriculture and Fisheries

Agriculture and fisheries remain central to Indonesia's rural economy and food security. Together, agriculture and fisheries account for roughly 12–14% of national GDP and employ nearly 30% of the workforce, with an even larger share in rural and resource-rich regions, according to official labor force statistics from Indonesia's Central Bureau of Statistics. Rice is the dominant staple crop, contributing more than half of total caloric intake, followed by maize, which is widely cultivated for both subsistence and local markets. Soybeans, although partly imported, play an important role in household diets and small-scale agro-processing. In parallel, Indonesia's extensive coastline supports one of the world's largest fisheries sectors, employing over 12 million workers directly and indirectly.[4] Coastal and nearshore fisheries are particularly important in eastern provinces such as Sulawesi and North Maluku, where fishing provides a primary source of income and protein for local communities. Because both agriculture and fisheries depend heavily on local natural capital—including forest cover, soil quality, freshwater availability, and coastal water conditions—they are especially vulnerable to environmental disturbances.

Table 3 examines how nickel mine openings affect local agricultural and fishery production within 30 km of mine sites, relative to nearby control areas. All specifications include climate controls and absorb grid-cell, mine-site, year-month, and province-by-year fixed effects, isolating changes in production associated with mine entry. Columns (1)–(3) document sizable declines in crop production following mine openings. Maize and rice output fall by approximately 12 percent, with effects that are statistically significant at conventional levels. In contrast, soybean production shows no statistically significant response, likely reflecting its more limited cultivation and weaker dependence on local land conditions in the affected regions. These patterns are consistent with earlier evidence on land degradation and suggest that mining-induced deforestation and soil disturbance translate into meaningful losses in

[4]See The Nature Conservancy for details.

agricultural productivity. Columns (4)–(5) report effects on fishery activity, measured by ship density and total fishing hours. Both indicators decline significantly after mine entry: ship density decreases by 0.001, and total fishing hours fall by 0.007. While modest in magnitude, these estimates are precisely estimated and economically meaningful given the low baseline levels of fishing activity. Moreover, these measures primarily capture registered and vessel-based fishing activity, and may understate impacts on small-scale and artisanal fisheries that are less likely to be recorded in ship-tracking data.[5] Taken together, the results indicate that environmental shocks induced by nickel mining disrupt local production systems across both terrestrial and marine sectors. Declines in agricultural and fishery output provide a key mechanism linking mining-driven environmental degradation to reductions in rural livelihoods and household welfare.

[Insert Table 3 here]

4.3 Impacts on Rural Household: Labor and Health

Table 4 reports baseline estimates of the impacts of nickel mining on village-level economic activities, environmental conditions, and public health outcomes. Columns (1)–(3) examine whether a village reports agriculture, fishing, or industry as its main source of income, respectively. Columns (4)–(6) focus on environmental pollution and health indicators, including reported soil or water pollution, the number of diarrhea cases, and the number of leptospirosis or cholera cases.

We find no statistically significant effects of mining exposure on whether villages rely primarily on agriculture, fishing, or industry as their main income source (Columns (1)–(3)). The estimated coefficients are small in magnitude and precisely estimated around zero, suggesting that mining expansion does not immediately alter the dominant sectoral classification of village livelihoods. This pattern is consistent with the idea that primary income structures adjust slowly and may mask underlying changes in productivity or labor allocation within sectors. In contrast, Column (4) shows a statistically significant increase in reported soil or water pollution following mine openings. Villages exposed to mining activity are more likely to report environmental contamination, consistent with land clearing, sediment runoff, and industrial discharge associated with open-pit mining. This result provides direct village-level

[5]Indonesia's coastal fisheries are dominated by small and artisanal vessels, many of which do not carry tracking devices and are therefore not fully captured in ship-density data. As a result, the estimated declines in fishing activity should be interpreted as a lower bound of the true impact.

evidence of environmental degradation in areas surrounding nickel mines. Columns (5) and (6) document adverse health impacts. We observe a significant increase in diarrhea incidence and a rise in cases of leptospirosis or cholera in exposed villages. These patterns are consistent with deteriorating water quality and heightened exposure to waterborne pathogens, linking environmental pollution to public health consequences.

[Insert Table 4 here]

The results indicate that while mining expansion does not immediately reshape villages' main income sources, it generates substantial environmental pollution and measurable health costs. These findings highlight an important disconnect between stable headline economic classifications and worsening local living conditions, underscoring the need to examine environmental and health externalities alongside conventional economic indicators.

5 Geopolitical Demand and Policy Amplification

Figure A3 provides a visual overview of the environmental changes associated with the expansion of nickel mining during the clean-energy transition. Comparing the early period (2012–2013) with the later period (2021–2022), the maps reveal pronounced increases in coastal water turbidity (KD490) and concurrent declines in vegetation cover (NDVI) around major nickel mining sites, suggesting substantial degradation of both marine and terrestrial ecosystems in exposed areas. To examine the drivers of this environmental intensification, Table 5 investigates how geopolitical demand shocks and policies—captured by global EV demand and Indonesia's 2020 nickel export ban—amplify the environmental and economic impacts of mining activity. Panel A focuses on global EV sales as a continuous measure of downstream demand, while Panel B exploits the 2020 export ban as a discrete industrial policy shock.

Panel A shows that higher global EV sales significantly intensify the environmental impacts of nickel mining. The interaction term between mining exposure and global EV sales is positive and statistically significant for ocean turbidity (Column (1)) and negative for forest cover (Column (2)). These results indicate that periods of stronger EV demand are associated with more severe coastal sedimentation and greater deforestation in areas surrounding mine sites. In contrast, the interaction effects on port activity and nighttime lights (Columns (3) and (4)) are statistically insignificant, suggesting that rising EV demand

does not primarily operate through short-run changes in local logistics intensity or general urban activity. Instead, Column (5) shows a large and statistically significant increase in new mine openings, indicating that global EV demand intensifies environmental impacts mainly by inducing extensive-margin expansion in mining activity. These results suggest that global EV demand amplifies environmental degradation not through increased utilization of existing infrastructure alone, but by accelerating the entry of new mining operations.

Panel B exploits Indonesia's 2020 export ban on unprocessed nickel ore, which sharply increased domestic processing incentives and the profitability of upstream extraction. The interaction between mining exposure and the post-2020 dummy shows a strong increase in ocean turbidity (Column (1)) and a significant decline in forest cover (Column (2)), consistent with intensified land clearing and sediment runoff following the policy change. Unlike the EV-demand channel, the export ban is also associated with sizable increases in nighttime lights (Column (4)) and new mine openings (Column (5)), pointing to a broader local economic response. The positive effect on nighttime lights suggests increased industrial and settlement activity around mining areas, while the surge in new mines confirms that the policy triggered a wave of mining expansion. Port activity (Column (3)) shows a positive but imprecisely estimated response, consistent with heterogeneous adjustments in logistics and export patterns during the transition period following the ban. While these policies have attracted substantial foreign direct investment into Indonesia's mining sector, the evidence suggests that this investment has not translated into cleaner extraction practices. Instead, foreign firms largely control the more advanced downstream technologies and processing activities, while Indonesia remains concentrated in the pollution-intensive upstream mining stages of global production networks. Consequently, the surge in mining activity following the 2020 export ban primarily increases extraction intensity in Indonesia, amplifying local environmental degradation rather than shifting production toward cleaner segments of the value chain.

[Insert Table 5 here]

6 Conclusion

This paper provides new evidence on how the expansion of nickel mining—driven jointly by rising global demand for electric vehicles and Indonesia's resource-based industrialization strategy—reshapes local environmental and socioeconomic conditions in mineral-producing

regions. Exploiting a staggered wave of nickel mine openings between 2012 and 2022 and combining high-resolution satellite data with village-level administrative statistics, I estimate causal effects on both terrestrial and marine ecosystems. Forest cover declines substantially around new extraction sites, while coastal sedimentation increases significantly. These environmental shocks translate into meaningful economic and welfare costs for nearby communities: agricultural and fisheries output fall, and village-level health outcomes deteriorate. Importantly, these externalities intensify during periods of rapid EV demand growth and following the tightening of Indonesia's nickel export ban in 2020. This pattern suggests that the costs of supplying the minerals that power the green transition are not fixed but increase with geopolitical competition.

These findings carry important policy implications for Indonesia. The country's nickel industrialization strategy has been effective in attracting foreign investment and positioning Indonesia as a key upstream hub in global EV battery and stainless-steel supply chains. However, the environmental and socioeconomic burdens of this transformation are borne disproportionately by rural and coastal communities located near extraction and processing sites. Strengthening regulatory oversight—particularly with respect to land conversion, water-quality monitoring, tailings management, and mine reclamation—would help mitigate these localized harms. Complementary policies that support affected households, including agricultural extension services, coastal ecosystem restoration, and targeted public-health interventions, are also important for offsetting welfare losses during periods of rapid industrial expansion.

The results highlight a governance challenge inherent in the global clean-energy transition. While the environmental benefits of decarbonization accrue globally, the environmental costs of extracting critical minerals remain highly localized and concentrated in resource-producing regions, particularly in the Global South. Existing international policy frameworks largely focus on securing mineral supply and reducing geopolitical risk but pay comparatively less attention to the environmental and social externalities generated upstream in extraction communities. Addressing this imbalance may require stronger forms of international coordination, including sustainability standards for mineral extraction, supply-chain due diligence requirements, and institutional arrangements that link downstream clean-energy deployment with upstream environmental safeguards.

Although this study focuses on Indonesia's nickel sector, the underlying mechanisms are likely to extend to a broader set of resource-rich economies participating in the global clean-energy transition. Many critical minerals essential for low-carbon technologies—such as lithium, cobalt, copper, and rare earths—are extracted predominantly in developing and

middle-income countries, but these countries differ substantially in governance capacity, institutional quality, and dependence on natural capital. In countries with relatively stronger regulatory capacity (e.g., Chile or parts of China), governments may be better able to internalize environmental costs through stricter permitting, monitoring, and enforcement. In contrast, in lower-capacity settings—such as parts of Sub-Saharan Africa or Southeast Asia—rapid mining expansion is more likely to outpace regulatory oversight, increasing the risk that environmental degradation translates directly into losses in agriculture, fisheries, and population health. These differences imply distinct policy priorities across levels of governance. At the national level, governments face the challenge of aligning industrial policy with environmental and social safeguards, ensuring that strategies to capture value from mineral resources incorporate environmental costs at the design stage rather than relying on ex post mitigation. At the subnational level, local governments play a critical role in enforcement and land-use management but often lack the fiscal and administrative capacity to regulate large-scale extraction, highlighting the need for stronger central–local coordination and capacity building. At the community level, where livelihoods remain closely tied to natural capital, policies that support adaptation—such as ecosystem restoration, sustainable fisheries management, and targeted public-health interventions—are essential to mitigate welfare losses.

References

Allcott, H. and D. Keniston (2018). Dutch disease or agglomeration? the local economic effects of natural resource booms in modern america. *The Review of Economic Studies 85*(2), 695–731.

Aragón, F. M. and J. P. Rud (2013). Natural resources and local communities: evidence from a peruvian gold mine. *American Economic Journal: Economic Policy 5*(2), 1–25.

Aragón, F. M. and J. P. Rud (2016). Polluting industries and agricultural productivity: Evidence from mining in ghana. *The Economic Journal 126*(597), 1980–2011.

Astuti, R., S. Raman, and A. E. Yeremia (2025). Putting community-centric justice into just transitions from the global south: the case of indonesia's nickel sector. *Environmental Research Letters 20*.

Baldwin, R. and R. Freeman (2022). Risks and global supply chains: What we know and what we need to know. *Annual Review of Economics 14*(1), 153–180.

Besley, T. and T. Persson (2023). The political economics of green transitions. *The Quarterly Journal of Economics 138*(3), 1863–1906.

Binding, C., J. Jerome, R. Bukata, and W. Booty (2010). Suspended particulate matter in lake erie derived from modis aquatic colour imagery. *International Journal of Remote Sensing 31*(19), 5239–5255.

Burgess, R., M. Hansen, B. A. Olken, P. Potapov, and S. Sieber (2012, 11). The political economy of deforestation in the tropics*. *The Quarterly Journal of Economics 127*(4), 1707–1754.

Caldara, D. and M. Iacoviello (2022). Measuring geopolitical risk. *American economic review 112*(4), 1194–1225.

Cloern, J. E. (2001). Our evolving conceptual model of the coastal eutrophication problem. *Marine ecology progress series 210*, 223–253.

Copeland, B. R. (2000). Trade and environment: policy linkages. *Environment and Development Economics 5*, 405 – 432.

Farrell, H. and A. L. Newman (2019). Weaponized interdependence: How global economic networks shape state coercion. *International security 44*(1), 42–79.

Gielen, D. (2021). Critical minerals for the energy transition. *International Renewable Energy Agency, Abu Dhabi 42*.

GONZÁLEZ-ESPINOSA, A. C., D. Borja, and J. Peña-Niño (2025). *People-powered energy transitions in resource-rich countries*. Natural Resource Governance Institute.

Gutman, G. and A. Ignatov (1998). The derivation of the green vegetation fraction from noaa/avhrr data for use in numerical weather prediction models. *International Journal of remote sensing 19*(8), 1533–1543.

Hansen, M. C., P. V. Potapov, R. Moore, M. Hancher, S. A. Turubanova, A. Tyukavina, D. Thau, S. V. Stehman, S. J. Goetz, T. R. Loveland, et al. (2013). High-resolution global maps of 21st-century forest cover change. *science 342*(6160), 850–853.

Kirk, J. T. (1994). *Light and photosynthesis in aquatic ecosystems*. Cambridge university press.

Lahadalia, B., C. Wijaya, T. Dartanto, and A. Subroto (2024). Nickel downstreaming in indonesia: Reinventing sustainable industrial policy and developmental state in building the ev industry in asean. *JAS (Journal of ASEAN Studies)*.

Levinson, A. and M. S. Taylor (2008). Unmasking the pollution haven effect. *International economic review 49*(1), 223–254.

Llamas-Orozco, J. A., F. Meng, G. S. Walker, A. F. Abdul-Manan, H. L. MacLean, I. D. Posen, and J. McKechnie (2023). Estimating the environmental impacts of global lithium-

ion battery supply chain: A temporal, geographical, and technological perspective. *PNAS nexus 2*(11), pgad361.

Lo, M. G., C. L. Morgans, T. Santika, S. Mumbunan, N. Winarni, J. Supriatna, M. Voigt, Z. G. Davies, and M. J. Struebig (2024). Nickel mining reduced forest cover in indonesia but had mixed outcomes for well-being. *One Earth 7*(11), 2019–2033.

Michaels, G. (2011). The long term consequences of resource-based specialisation. *The Economic Journal 121*(551), 31–57.

Nygaard, A. (2022). The geopolitical risk and strategic uncertainty of green growth after the ukraine invasion: How the circular economy can decrease the market power of and resource dependency on critical minerals. *Circular Economy and Sustainability 3*, 1099–1126.

Ou, S., X. Hao, Z. Lin, H. Wang, J. Bouchard, X. He, S. Przesmitzki, Z. Wu, J. Zheng, R. Lv, et al. (2019). Light-duty plug-in electric vehicles in china: An overview on the market and its comparisons to the united states. *Renewable and Sustainable Energy Reviews 112*, 747–761.

Overland, I. (2019). The geopolitics of renewable energy: Debunking four emerging myths. *Energy research & social science 49*, 36–40.

Peñaloza-Pacheco, L., V. Triantafyllou, and G. Martínez (2025). The non-green effects of going green: Local environmental and economic consequences of lithium extraction in chile. *Journal of Environmental Economics and Management*.

Qin, X., B. Wu, H. Zeng, M. Zhang, and F. Tian (2023). Ggcp10: A global gridded crop production dataset at 10km resolution from 2010 to 2020. *Earth System Science Data Discussions 2023*, 1–44.

Ramadhani, E. and A. K. Paksi (2025a). The price of progress: An assessment of indonesia's nickel downstreaming policy for the global energy transition. In *BIO Web of Conferences*, Volume 199, pp. 02002. EDP Sciences.

Ramadhani, E. and A. K. Paksi (2025b). The price of progress: An assessment of indonesia's nickel downstreaming policy for the global energy transition. *BIO Web of Conferences*.

Shen, Y., X. Shi, Z. Zhao, R. Q. Grafton, J. Yu, and Y. Shan (2024). Quantifying energy transition vulnerability helps more just and inclusive decarbonization. *PNAS nexus 3*(10), pgae427.

Specker, A., R. Gilli, E. Di Francesco, S. Manoochehri, R. Zoboli, G. Marin, S. Tagliapietra, P. Jensen, and B. Vidal (2024). Environmental impact of material supply chain disruptions. *European Environment Agency. European Topic Centre. Circular Economy and Resource Use*.

Tanaka, S., K. Teshima, and E. Verhoogen (2022). North-south displacement effects of environmental regulation: The case of battery recycling. *American Economic Review: Insights 4*(3), 271–288.

Udeaja, E. A., J. M. Tule, S. S. Akadiri, E. O. Akanni, and P. F. Offum (2024). Do economic policy uncertainty and geopolitical risk impede economic transformation? evidence from resource rich country. *Journal of Economics and Finance 48*, 1145 – 1165.

Von der Goltz, J. and P. Barnwal (2019). Mines: The local wealth and health effects of mineral mining in developing countries. *Journal of Development Economics 139*, 1–16.

Xie, V. W., W. You, and R. Goldblatt (2025). Investor origin and deforestation: Evidence from global mining sites. *Review of Economics and Statistics*, 1–28.

Zamanillo, E. and M. Rivera (2025). *Mining Is Dead. Long Live Geopolitical Mining: How China's Critical Minerals Strategy Is Reshaping the New World Order*. QM Books.

Tables and Figures

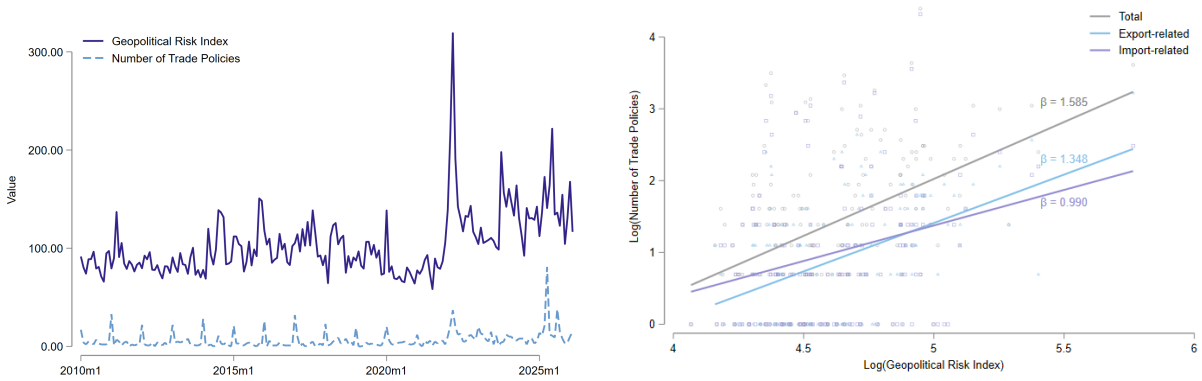

Figure 1: Geopolitical Risk and Trade Policy Interventions

Notes: The Geopolitical Risk (GPR) Index is from Caldara and Iacoviello (2022). Trade policy interventions are obtained from the Global Trade Alert (GTA), which records event-level import and export policy measures on critical minerals. We aggregate these interventions to the monthly level.

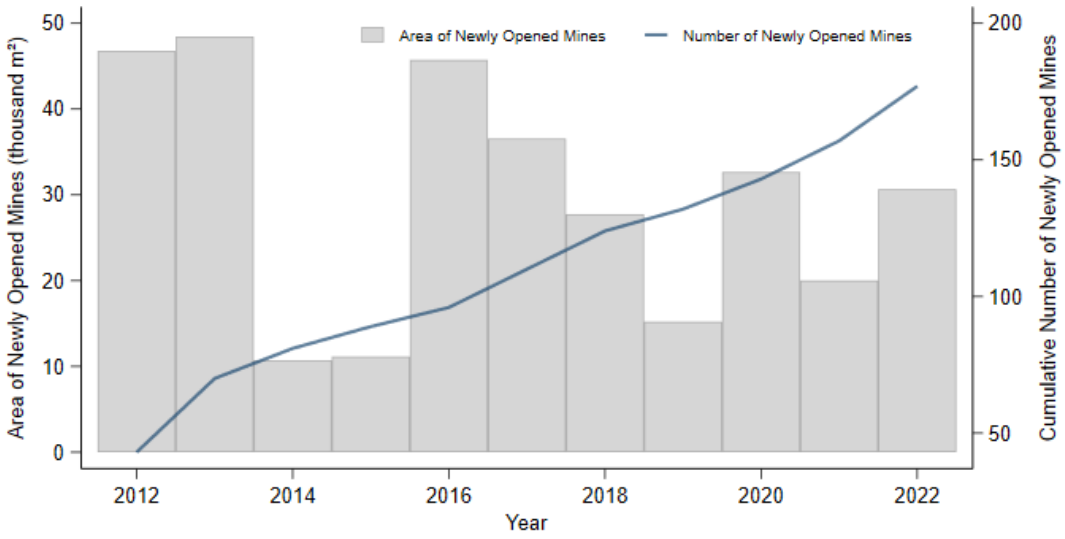

Figure 2: Trends in Newly Opened Mines and Mining Area

Notes: The figure shows the cumulative number of newly opened mines and the annual total area of newly opened mines between 2012 and 2022.

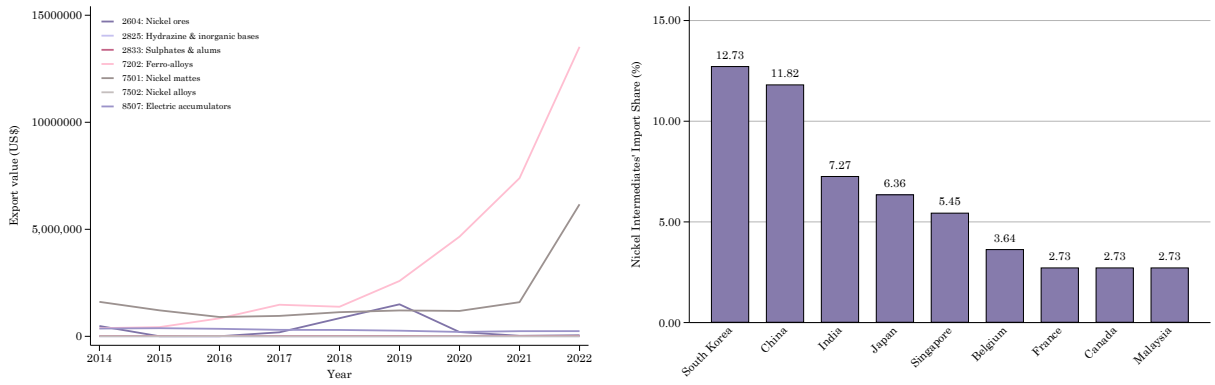

Figure 3: Indonesia Export of Nickel Ore and Related Products

Notes: Indonesia's annual trade flows are sourced from the CEPII BACI International Trade Database, which harmonizes bilateral trade data from UN Comtrade at the HS product level across all importers and exporters.

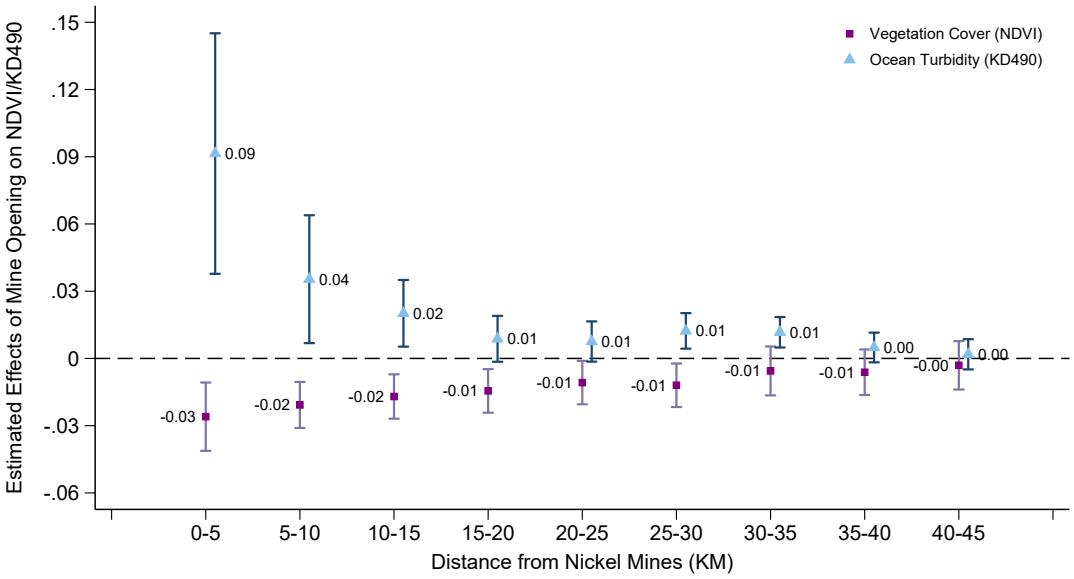

Figure 4: Environmental Impacts from Nickel Mine Openings of Different Treatment Groups

Notes: This figure displays the effects of nickel mine openings on vegetation cover and ocean turbidity across distance-based treatment bands. Treatment groups are defined by grid cells located within successive 5 km intervals from 0–5 km, 5-10 km, ..., 40–45 km of the nearest mining site, with areas beyond 45 km serving as the reference group. The dependent variables are the natural logarithm of monthly NDVI (vegetation cover) and KD490 (ocean turbidity) over the period 2012–2022. The sample is restricted to observations within 50 km of mining sites. All regressions control for climatic conditions and include grid fixed effects, mine-site fixed effects, year-month fixed effects, and province-by-year fixed effects. Standard errors are clustered at the grid level. Error bars represent 95 percent confidence intervals.

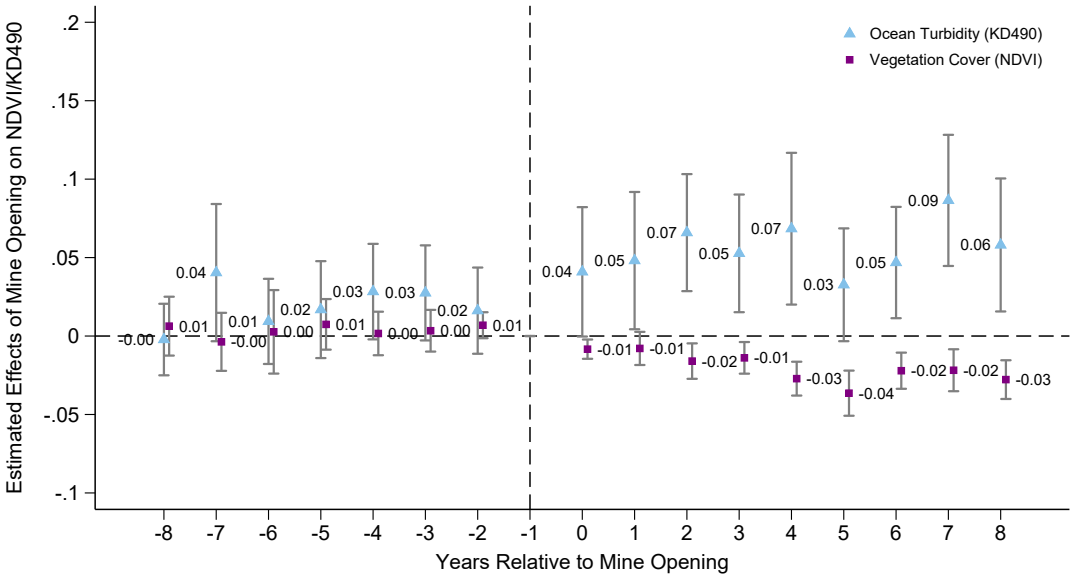

Figure 5: Event Study of Mine Opening on Ocean Turbidity and Vegetation Cover

Notes: This figure shows event-study estimates of the effects of nickel mine openings on ocean turbidity (KD490) and vegetation cover (NDVI). Coefficients are plotted relative to the year of mine opening, with error bars indicating 95% confidence intervals. All regressions control for climatic conditions and include grid fixed effects, mine-site fixed effects, year-month fixed effects, and province-by-year fixed effects. Standard errors are clustered at the grid level.

Table 1: Baseline Estimate on Forest Cover and Water Quality

	(1)	(2)	(3)	(4)
Panel A: Vegetation Index				
Treat ∗ Post	-0.018***	-0.018***	-0.017***	-0.020***
	(0.006)	(0.006)	(0.005)	(0.007)
Observations	198271	198271	198271	150243
R2	0.75	0.75	0.76	0.76
Mean Dep Variable	0.81	0.81	0.81	0.81
Panel B: Ocean Color				
Treat ∗ Post	0.022**	0.022**	0.028***	0.025***
	(0.009)	(0.009)	(0.008)	(0.008)
Observations	544496	544496	544496	216363
R2	0.73	0.73	0.74	0.73
Mean Dep Variable	0.05	0.05	0.05	0.05
Grid cell FE	Y	Y	Y	Y
Year-month FE	Y	Y	Y	Y
Mine FE		Y	Y	Y
Province-by-year FE			Y	Y
Control group	30-100km	30-100km	30-100km	30-50km

Notes: *P $<$ 0.10; **P $<$ 0.05; ***P $<$ 0.01. The dependent variables are the natural logarithms of monthly NDVI and ocean turbidity (KD490) from 2012 to 2022. Samples used to generate the estimates reported in Columns (1)–(3) are restricted to grid cells within 100 km of the nearest nickel mine site; Column (4) further restricts the sample to grid cells within 50 km. In Panel A, regressions include climate control variables: temperature, dew point, wind speed, precipitation, and visibility, along with their second-order polynomials. In Panel B, in addition to the climate controls, we also control for oceanographic conditions, including current speed, current direction, sea surface temperature, salinity, mixed-layer thickness, sea surface height, and second-order polynomials. All specifications have grid fixed effects, mine-site fixed effects, year-month fixed effects, and province-by-year fixed effects. Standard errors are clustered at the grid level. Detailed regression results are reported in Tables A1 and A2 in the Appendix.

Table 2: Robustness Check on Forest Cover and Water Quality

	(1) Baseline	(2) Remove outliers	(3) Placebo test	(4) HAC cluster	(5) CSDID
Panel A: Vegetation Index					
Treat ∗ Post	-0.020***	-0.020***	0.003	-0.020***	-0.014 **
	(0.007)	(0.007)	(0.003)	(0.002)	(0.007)
Observations	150243	150243	167187	150243	11330
R2	0.76	0.77	0.67		
Mean Dep Variable	0.81	0.81	0.74	0.81	
Panel B: Ocean Color					
Treat ∗ Post	0.025***	0.024***	0.003	0.025*	0.033***
	(0.008)	(0.008)	(0.009)	(0.014)	0.008
Observations	216363	216363	144789	216363	19497
R2	0.73	0.74	0.86		
Mean Dep Variable	0.05	0.05	0.15	0.05	

Notes: *P $<$ 0.10; **P $<$ 0.05; ***P $<$ 0.01. The dependent variables are the natural logarithms of monthly NDVI (vegetation cover) and KD490 (ocean turbidity) from 2012 to 2022. Samples used to generate the reported estimates are restricted to grid cells within 50 km of the nearest nickel mine site. Column (2) removes the top and bottom 1% of observations as outliers; Column (3) re-estimates the effects using non-metal mine openings as a placebo test; Column (4) adopts a Conley (HAC) spatial standard error correction; and Column (5) reports estimates from the CSDID approach. In Panel A, regressions include climate control variables: temperature, dew point, wind speed, precipitation, and visibility, along with their second-order polynomials. In Panel B, in addition to the climate controls, we also control for oceanographic conditions, including current speed, current direction, sea surface temperature, salinity, mixed-layer thickness, sea surface height, and second-order polynomials. All specifications have grid fixed effects, mine-site fixed effects, year-month fixed effects, and province-by-year fixed effects. Standard errors are clustered at the grid level. Detailed regression results are reported in Tables A3 and A4 in the Appendix.

Table 3: Baseline Estimate on Agricultural and Fishery Production

	(1)	(2)	(3)	(4)	(5)
	Logarithm of Production			**Fishing Variable**	
	Maize	Rice	Soybean	Ship density	Total hours
Treat $*$ **Post**	-0.119***	-0.120**	0.112	-0.001**	-0.007*
	(0.044)	(0.057)	(0.090)	(0.001)	(0.004)
Observations	2077	2075	2160	494016	494016
R2	0.90	0.92	0.96	0.04	0.05
Mean Dep Variable	0.78	2.03	0.11	0.00	0.01

Notes: *P $<$ 0.10; **P $<$ 0.05; ***P $<$ 0.01. The dependent variables are the natural logarithms of annual agricultural production from 2010 to 2022 and monthly fishery variables from 2012 to 2022. Samples used to generate the reported estimates are restricted to grid cells within 50 km of the nearest nickel mine site. All specifications include climate controls, grid fixed effects, mine-site fixed effects, year-month fixed effects, and province-by-year fixed effects. Standard errors are clustered at the grid level. Detailed regression results are reported in Table A5 in the Appendix.

Table 4: Baseline Estimate on Village Outcomes

	(1)	(2)	(3)	(4)	(5)	(6)
	Source income agriculture	Source income fishing	Source income industry	Pollution from soil/water	Number of diarrhea	Number of leptospirosis/cholera
Treat $*$ **Post**	0.001	-0.000	0.017	0.200**	0.301*	0.059**
	(0.050)	(0.017)	(0.049)	(0.085)	(0.173)	(0.030)
Observations	4889	4889	4889	4889	4889	4889
R2	0.88	0.96	0.51	0.67	0.50	0.97
Mean Dep Variable	0.90	0.01	0.03	0.03	0.30	1.03

Notes: *P $<$ 0.10; **P $<$ 0.05; ***P $<$ 0.01. The dependent variables are the natural logarithms of annual agricultural production from 2010 to 2022 and monthly fishery variables in 2018 and 2021. Samples used to generate the reported estimates are restricted to villages within 50 km of the nearest nickel mine site. All specifications include climate controls, village fixed effects, mine-site fixed effects, year fixed effects, and province-by-year fixed effects. Standard errors are clustered at the grid level. Detailed regression results are reported in Table A6 in the Appendix.

Table 5: Intensification of Global EV Demand and Export Ban Policies

	(1) Ocean turbidity	(2) Forest cover	(3) Port activity	(4) Night light	(5) New mines
Panel A: Global EV Sales					
Treat*Post	0.002	-0.010	-0.098	-0.159	0.400***
	(0.007)	(0.007)	(0.175)	(0.202)	(0.150)
Treat * Post * EVsales	0.012***	-0.004***	0.006	0.017	0.115***
	(0.003)	(0.001)	(0.060)	(0.048)	(0.030)
Observations	216363	150243	37267	410850	3052
R2	0.74	0.76	0.79	0.66	0.77
Mean Dep Variable	0.05	0.81	8.41	0.33	10.04
Panel B: Export Ban in 2020					
Treat*Post	0.007	-0.012*	-0.044	-0.017	0.482***
	(0.007)	(0.006)	(0.189)	(0.173)	(0.142)
Treat * Post * Dummy2020	0.060***	-0.023***	0.338**	0.582*	0.339**
	(0.012)	(0.005)	(0.151)	(0.321)	(0.139)
Observations	216363	150243	37267	410850	3052
R2	0.74	0.76	0.79	0.65	0.77
Mean Dep Variable	0.05	0.81	8.41	0.33	10.04

Notes: *P $<$ 0.10; **P $<$ 0.05; ***P $<$ 0.01. The dependent variables are ocean turbidity (KD490), vegetation cover (NDVI), port activity, nighttime light intensity, and the number of newly opened mines from 2012-2022. Samples used to generate the reported estimates are restricted to grid cells within 50 km of the nearest nickel mine site. $EVsales$ denotes annual global electric vehicle demand, while $Dummy2020$ is an indicator variable equal to one in the post-2020 export ban period. All specifications include climate controls, grid fixed effects, mine-site fixed effects, year-month fixed effects, and province-by-year fixed effects. Standard errors are clustered at the grid level.

Appendix

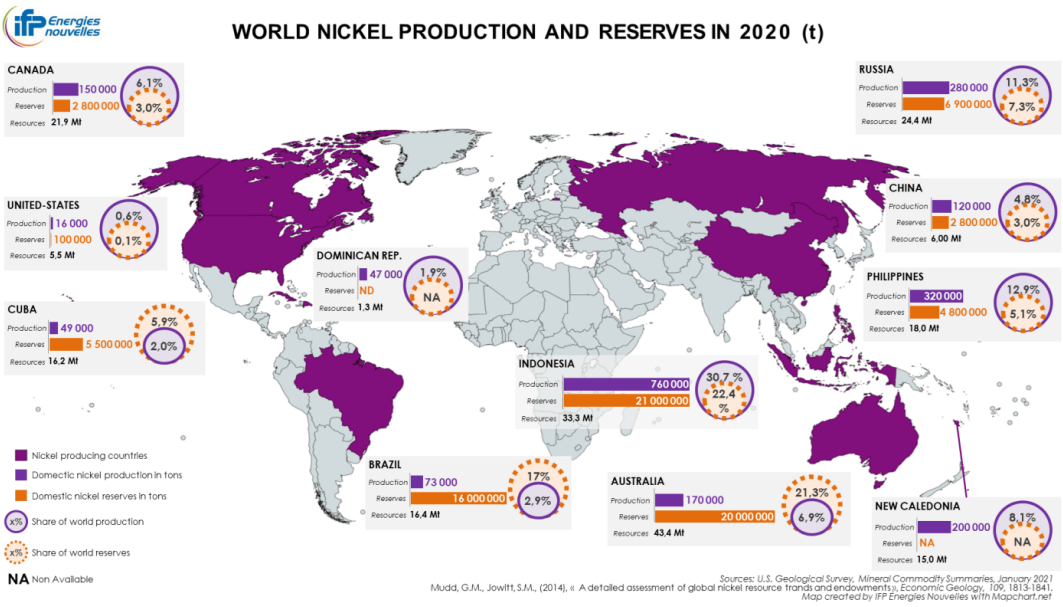

Figure A1: Global Nickel Production in 2020

Figure A2: Nickel Mining Sites in Indonesia

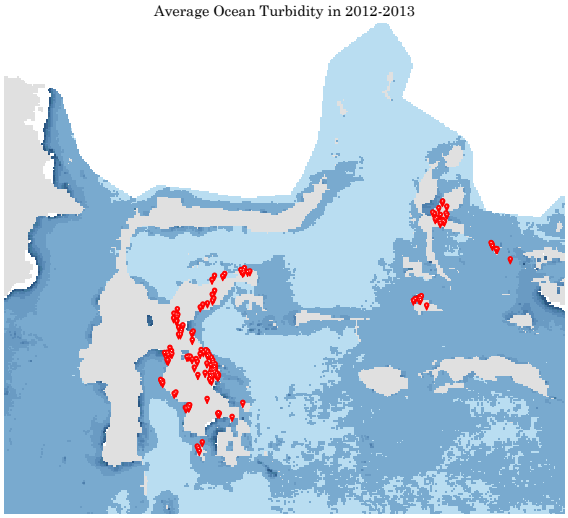

a: Average KD490 in 2012-2013

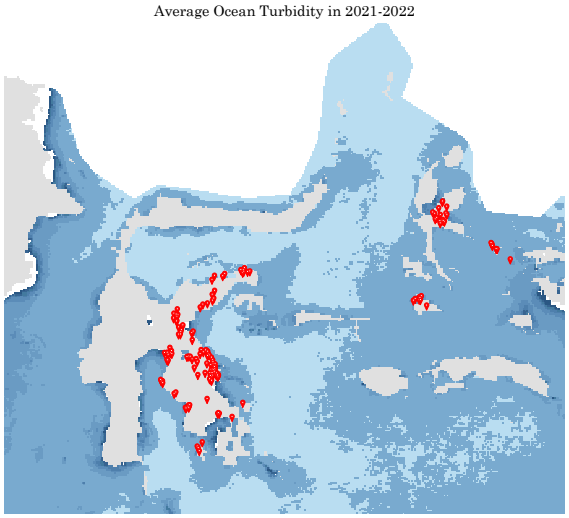

b: Average KD490 in 2021-2022

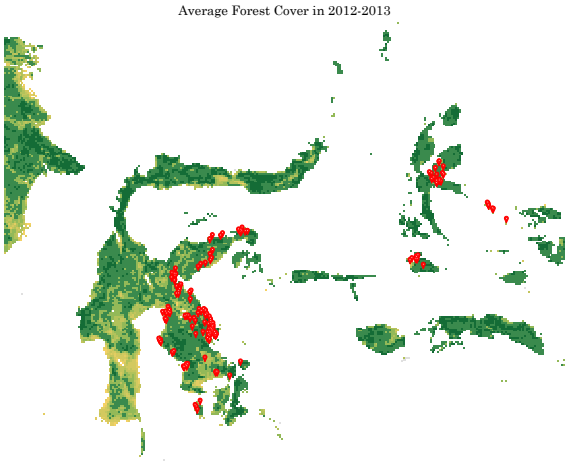

c: Average NDVI in 2012-2013

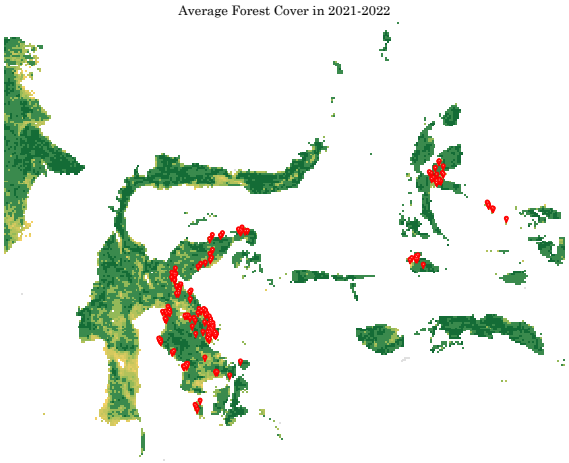

d: Average NDVI in 2021-2022

Figure A3: Spatial Patterns of Coastal Water Turbidity and Vegetation Cover around Nickel Mining Regions in Indonesia

Notes: This figure maps average ocean turbidity (KD490) and vegetation cover (NDVI) around nickel mining regions in Indonesia before and after the expansion of mining activity. Panels (a) and (b) show average KD490 in 2012–2013 and 2021–2022, respectively, where higher values indicate increased coastal water turbidity. Panels (c) and (d) display average NDVI over the same periods, with lower values indicating reduced vegetation cover. Red points denote the locations of nickel mines.

Table A1: Baseline Estimate on Vegetation Cover

	(1)	(2)	(3)	(4)
Panel A: Vegetation Index				
Treat	0.000	0.000	0.000	0.000
	(.)	(.)	(.)	(.)
Post	0.007	0.007	0.008**	0.011**
	(0.004)	(0.004)	(0.003)	(0.005)
Treat * Post	-0.018***	-0.018***	-0.017***	-0.020***
	(0.006)	(0.006)	(0.005)	(0.007)
Temperature	0.164***	0.164***	0.180***	0.179***
	(0.057)	(0.057)	(0.049)	(0.050)
Dew point	-0.083	-0.083	-0.138***	-0.139***
	(0.052)	(0.052)	(0.046)	(0.047)
Wind speed	-0.005	-0.005	0.003	0.003
	(0.016)	(0.016)	(0.016)	(0.016)
Precipitation	-0.027	-0.027	-0.042	-0.042
	(0.023)	(0.023)	(0.026)	(0.026)
Temperature square	-0.001***	-0.001***	-0.001***	-0.001***
	(0.000)	(0.000)	(0.000)	(0.000)
Dew point square	0.001	0.001	0.001***	0.001***
	(0.000)	(0.000)	(0.000)	(0.000)
Wind speed square	-0.000	-0.000	-0.000	-0.000
	(0.002)	(0.002)	(0.002)	(0.002)
Precipitation square	-0.007	-0.007	0.007	0.006
	(0.032)	(0.032)	(0.039)	(0.039)
Visibility square	0.013***	0.013***	0.014***	0.014***
	(0.005)	(0.005)	(0.005)	(0.005)
Visibility	-0.147***	-0.147***	-0.155***	-0.156***
	(0.054)	(0.054)	(0.058)	(0.058)
Sea level pressure	2.682	2.682	1.472	1.471
	(2.285)	(2.286)	(2.228)	(2.231)
Sea level pressure square	-0.001	-0.001	-0.001	-0.001
	(0.001)	(0.001)	(0.001)	(0.001)
Constant	-1347.754	-1347.754	-737.901	-737.572
	(1152.312)	(1152.684)	(1124.338)	(1125.980)
Observations	198271	198271	198271	150243
R2	0.75	0.75	0.76	0.76
Mean Dep Variable	0.81	0.81	0.81	0.81
Grid cell FE	Y	Y	Y	Y
Year-month FE	Y	Y	Y	Y
Mine FE		Y	Y	Y
Province-by-year FE			Y	Y
Control group	30-100km	30-100km	30-100km	30-50km

Notes: *P < 0.10; **P < 0.05; ***P < 0.01. The dependent variables are the natural logarithms of monthly NDVI from 2012 to 2022. Samples used to generate the estimates reported in Columns (1)–(3) are restricted to grid cells within 100 km of the nearest nickel mine site; Column (4) further restricts the sample to grid cells within 50 km. In Panel A, regressions include climate control variables: temperature, dew point, wind speed, precipitation, and visibility, along with their second-order polynomials. All specifications have grid fixed effects, mine-site fixed effects, year-month fixed effects, and province-by-year fixed effects. Standard errors are clustered at the grid level.

Table A2: Baseline Estimate on Water Quality

	(1)	(2)	(3)	(4)
Panel B: Ocean Turbidity				
Treat	0.000	0.000	0.000	0.000
	(.)	(.)	(.)	(.)
Post	0.006	0.006	0.010*	0.013*
	(0.008)	(0.008)	(0.006)	(0.007)
Treat * Post	0.022**	0.022**	0.028***	0.025***
	(0.009)	(0.009)	(0.008)	(0.008)
Current speed	0.046	0.046	0.028	0.029
	(0.049)	(0.049)	(0.044)	(0.057)
Current direction	0.000	0.000	0.000	0.000
	(0.000)	(0.000)	(0.000)	(0.000)
Sea water temperature	-3.238***	-3.238***	-2.962***	-2.927***
	(0.154)	(0.154)	(0.161)	(0.192)
Sea water salinity	-0.277***	-0.277***	-0.294***	-0.294***
	(0.060)	(0.060)	(0.064)	(0.068)
Mixed layer thickness	-0.012***	-0.012***	-0.012***	-0.011***
	(0.002)	(0.002)	(0.002)	(0.002)
Sea surface height	-4.560***	-4.560***	-9.472***	-9.260***
	(0.717)	(0.717)	(1.441)	(1.528)
Temperature	-0.579***	-0.579***	-0.556***	-0.531***
	(0.113)	(0.113)	(0.113)	(0.124)
Dew point	0.042	0.042	-0.054	-0.096
	(0.128)	(0.128)	(0.138)	(0.143)
Wind speed	-0.313***	-0.313***	-0.265***	-0.277***
	(0.039)	(0.039)	(0.032)	(0.031)
Precipitation	-0.023	-0.023	-0.114	-0.104
	(0.075)	(0.075)	(0.071)	(0.080)
Temperature square	0.003***	0.003***	0.003***	0.003***
	(0.001)	(0.001)	(0.001)	(0.001)
Dew point square	0.000	0.000	0.001	0.001
	(0.001)	(0.001)	(0.001)	(0.001)
Wind speed square	0.046***	0.046***	0.041***	0.042***
	(0.006)	(0.006)	(0.006)	(0.006)
Precipitation square	0.194	0.194	0.293***	0.267**
	(0.119)	(0.119)	(0.111)	(0.123)
Visibility square	0.122***	0.122***	0.135***	0.143***
	(0.026)	(0.026)	(0.027)	(0.029)
Visibility	-1.328***	-1.328***	-1.508***	-1.598***
	(0.286)	(0.286)	(0.293)	(0.316)
Sea level pressure	28.011***	28.011***	31.287***	30.167***
	(4.995)	(4.995)	(4.439)	(4.783)
Sea level pressure square	-0.014***	-0.014***	-0.015***	-0.015***
	(0.002)	(0.002)	(0.002)	(0.002)
Current speed square	-0.093*	-0.093*	-0.053	-0.087
	(0.048)	(0.048)	(0.042)	(0.067)
Current direction square	-0.000	-0.000	-0.000	-0.000
	(0.000)	(0.000)	(0.000)	(0.000)
Sea water temperature square	0.054***	0.054***	0.049***	0.049***
	(0.003)	(0.003)	(0.003)	(0.003)
Sea water salinity square	0.004***	0.004***	0.005***	0.005***
	(0.001)	(0.001)	(0.001)	(0.001)
Mixed layer thickness square	0.000***	0.000***	0.000***	0.000***
	(0.000)	(0.000)	(0.000)	(0.000)
Sea surface height square	2.626***	2.626***	6.151***	6.117***
	(0.532)	(0.532)	(1.000)	(1.067)
Constant	-14080.347***	-14080.347***	-15739.398***	-15175.498***
	(2523.097)	(2523.234)	(2239.657)	(2413.325)
Observations	544496	544496	544496	216363
R2	0.73	0.73	0.74	0.73
Mean Dep Variable	0.05	0.05	0.05	0.05
Grid cell FE	Y	Y	Y	Y
Year-month FE	Y	Y	Y	Y
Mine FE		Y	Y	Y
Province-by-year FE			Y	Y
Control group	30-100km	30-100km	30-100km	30-50km

Notes: *P < 0.10; **P < 0.05; ***P < 0.01. The dependent variables are the natural logarithms of monthly ocean turbidity (KD490) from 2012 to 2022. Samples used to generate the estimates reported in Columns (1)–(3) are restricted to grid cells within 100 km of the nearest nickel mine site; Column (4) further restricts the sample to grid cells within 50 km. In Panel B, in addition to the climate

Table A3: Robustness Check on Forest Cover

	(1) Baseline	(2) Remove outliers	(3) Placebo test	(4) HAC cluster	(5) CSDID
Panel A: Vegetation Cover					
Treat	0.000	0.000	0.000		
	(.)	(.)	(.)		
Post	0.011**	0.011**	-0.004		
	(0.005)	(0.004)	(0.005)		
Treat ∗ Post	-0.020***	-0.020***	0.003	-0.020***	
	(0.007)	(0.007)	(0.003)	(0.002)	
Temperature	0.179***	0.183***	0.449**		
	(0.050)	(0.048)	(0.198)		
Dew point	-0.139***	-0.135***	0.262***		
	(0.047)	(0.046)	(0.079)		
Wind speed	0.003	0.004	0.001		
	(0.016)	(0.017)	(0.013)		
Precipitation	-0.042	-0.045*	-0.059*		
	(0.026)	(0.025)	(0.036)		
Temperature square	-0.001***	-0.001***	-0.003**		
	(0.000)	(0.000)	(0.001)		
Dew point square	0.001***	0.001***	-0.002***		
	(0.000)	(0.000)	(0.001)		
Wind speed square	-0.000	-0.001	-0.000		
	(0.002)	(0.002)	(0.001)		
Precipitation square	0.006	0.013	0.013		
	(0.039)	(0.037)	(0.042)		
Visibility square	0.014***	0.014***	-0.002		
	(0.005)	(0.005)	(0.002)		
Visibility	-0.156***	-0.156***	-0.003		
	(0.058)	(0.058)	(0.018)		
Sea level pressure	1.471	1.623	9.187*		
	(2.231)	(2.243)	(5.159)		
Sea level pressure square	-0.001	-0.001	-0.005*		
	(0.001)	(0.001)	(0.003)		
Constant	-737.572	-814.302	-4662.651*		
	(1125.980)	(1131.939)	(2608.212)		
Observations	150243	150243	167187	150243	
R2	0.76	0.77	0.67	0.00	
Mean Dep Variable	0.81	0.81	0.74	0.81	

Notes: *P < 0.10; **P < 0.05; ***P < 0.01. The dependent variables are the natural logarithms of monthly vegetation cover(NDVI) from 2012 to 2022. Samples used to generate the reported estimates are restricted to grid cells within 50 km of the nearest nickel mine site. Column (2) removes the top and bottom 1% of observations as outliers; Column (3) re-estimates the effects using non-metal mine openings as a placebo test; Column (4) adopts a Conley (HAC) spatial standard error correction; and Column (5) reports estimates from the CSDID approach. In Panel A, regressions include climate control variables: temperature, dew point, wind speed, precipitation, and visibility, along with their second-order polynomials. All specifications have grid fixed effects, mine-site fixed effects, year-month fixed effects, and province-by-year fixed effects. Standard errors are clustered at the grid level.

Table A4: Robustness Check on Water Quality

	(1) Baseline	(2) Remove outliers	(3) Placebo test	(4) HAC cluster	(5) CSDID
Panel B: Ocean Turbidity					
Treat	0.000	0.000	0.000		
	(.)	(.)	(.)		
Post	0.013*	0.013*	-0.012		
	(0.007)	(0.007)	(0.012)		
Treat ∗ Post	0.025***	0.024***	0.003	0.025*	
	(0.008)	(0.008)	(0.009)	(0.014)	
Current speed	0.029	0.030	0.484***		
	(0.057)	(0.057)	(0.062)		
Current direction	0.000	0.000	0.001***		
	(0.000)	(0.000)	(0.000)		
Sea water temperature	-2.927***	-2.932***	-3.648***		
	(0.192)	(0.192)	(0.142)		
Sea water salinity	-0.294***	-0.293***	-0.286***		
	(0.068)	(0.068)	(0.109)		
Mixed layer thickness	-0.011***	-0.011***	0.003		
	(0.002)	(0.002)	(0.003)		
Sea surface height	-9.260***	-9.357***	-3.303***		
	(1.528)	(1.515)	(0.343)		
Temperature	-0.531***	-0.541***	2.459***		
	(0.124)	(0.124)	(0.219)		
Dew point	-0.096	-0.091	-0.448***		
	(0.143)	(0.143)	(0.130)		
Wind speed	-0.277***	-0.276***	-0.109***		
	(0.031)	(0.031)	(0.020)		
Precipitation	-0.104	-0.103	-0.090		
	(0.080)	(0.080)	(0.081)		
Temperature square	0.003***	0.003***	-0.015***		
	(0.001)	(0.001)	(0.001)		
Dew point square	0.001	0.001	0.003***		
	(0.001)	(0.001)	(0.001)		
Wind speed square	0.042***	0.042***	0.007***		
	(0.006)	(0.006)	(0.002)		
Precipitation square	0.267**	0.265**	0.774***		
	(0.123)	(0.122)	(0.165)		
Visibility square	0.143***	0.143***	-0.000		
	(0.029)	(0.029)	(0.006)		
Visibility	-1.598***	-1.600***	0.008		
	(0.316)	(0.316)	(0.059)		
Sea level pressure	30.167***	29.876***	3.209		
	(4.783)	(4.784)	(8.534)		
Sea level pressure square	-0.015***	-0.015***	-0.002		
	(0.002)	(0.002)	(0.004)		
Current speed square	-0.087	-0.088	-0.446***		
	(0.067)	(0.067)	(0.071)		
Current direction square	-0.000	-0.000	-0.000***		
	(0.000)	(0.000)	(0.000)		
Sea water temperature square	0.049***	0.049***	0.062***		
	(0.003)	(0.003)	(0.002)		
Sea water salinity square	0.005***	0.005***	0.003		
	(0.001)	(0.001)	(0.002)		
Mixed layer thickness square	0.000***	0.000***	0.000		
	(0.000)	(0.000)	(0.000)		
Sea surface height square	6.117***	6.191***	1.582***		
	(1.067)	(1.059)	(0.219)		
Constant	-15175.498***	-15028.230***	-1667.953		
	(2413.325)	(2413.711)	(4308.000)		
Observations	216363	216363	144789	216363	
R2	0.73	0.74	0.86	0.00	
Mean Dep Variable	0.05	0.05	0.15	0.05	

Notes: *P < 0.10; **P < 0.05; ***P < 0.01. The dependent variables are the natural logarithms of monthly ocean turbidity (KD490) from 2012 to 2022. Samples used to generate the reported estimates are restricted to grid cells within 50 km of the nearest nickel mine site. Column (2) removes the top and bottom 1% of observations as outliers; Column (3) re-estimates the effects using non-metal mine openings as a placebo test; Column (4) adopts a Conley (HAC) spatial standard error correction; and Column (5) reports estimates from the CSDID approach. In Panel B, in addition to the climate controls, we also control for oceanographic conditions, including current speed, current direction, sea surface temperature, salinity, mixed-layer thickness, sea surface height, and second-order polynomials. All specifications have grid fixed effects, mine-site fixed effects, year-month fixed effects, and province-by-year fixed effects. Standard errors are clustered at the grid level.

Table A5: Baseline Estimate on Agricultural and Fishery Production

	(1)	(2)	(3)	(4)	(5)
	Logarithm of Production			**Fishing Variable**	
	Maize	Rice	Soybean	Ship density	Total hours
Treat	0.000	0.000	0.000	0.000	0.000
	(.)	(.)	(.)	(.)	(.)
Post	0.015	0.149	-0.283*	0.001**	-0.008
	(0.047)	(0.099)	(0.163)	(0.001)	(0.006)
Treat * Post	-0.119***	-0.120**	0.112	-0.001**	-0.007*
	(0.044)	(0.057)	(0.090)	(0.001)	(0.004)
Temperature	-9.799	29.963	13.389	-0.011	-0.057
	(8.781)	(21.563)	(12.783)	(0.008)	(0.136)
Dew point	13.446	19.346	-40.963		
	(13.464)	(18.021)	(26.007)		
Wind speed	-0.214	0.435	0.180	-0.001	-0.007
	(0.806)	(1.353)	(0.751)	(0.002)	(0.045)
Precipitation	-4.740	-0.085	12.240**	0.014	0.223
	(3.059)	(4.217)	(6.184)	(0.010)	(0.182)
Temperature square	0.059	-0.182	-0.082	0.000	0.000
	(0.053)	(0.131)	(0.078)	(0.000)	(0.001)
Dew point square	-0.090	-0.129	0.274		
	(0.091)	(0.121)	(0.174)		
Wind speed square	0.015	-0.074	-0.024	-0.000	-0.004
	(0.113)	(0.203)	(0.110)	(0.000)	(0.005)
Precipitation square	11.183	5.172	-33.417**	-0.019*	-0.287
	(7.476)	(12.127)	(15.049)	(0.012)	(0.215)
Visibility	-5.367**	0.975	5.811		
	(2.669)	(4.097)	(5.206)		
Visibility square	0.474**	-0.162	-0.505		
	(0.238)	(0.375)	(0.474)		
Sea level pressure	-12.032	411.625**	74.008	-1.662**	-27.735
	(98.197)	(206.880)	(186.597)	(0.845)	(16.968)
Sea level pressure square	0.006	-0.204**	-0.037	0.001**	0.014
	(0.049)	(0.102)	(0.092)	(0.000)	(0.008)
Constant	6048.141	-210011.349**	-36395.358	839.795**	14017.121
	(49552.496)	(105564.329)	(94635.396)	(427.162)	(8576.325)
Observations	2077	2075	2160	494016	494016
R2	0.90	0.92	0.96	0.04	0.05
Mean Dep Variable	0.78	2.03	0.11	0.00	0.01

Notes: *P < 0.10; **P < 0.05; ***P < 0.01. The dependent variables are the natural logarithms of annual agricultural production from 2010 to 2022 and monthly fishery variables from 2012 to 2022. Samples used to generate the reported estimates are restricted to grid cells within 50 km of the nearest nickel mine site. All specifications include climate controls, grid fixed effects, mine-site fixed effects, year-month fixed effects, and province-by-year fixed effects. Standard errors are clustered at the grid level.

Table A6: Baseline Estimate on Village Outcomes

	(1)	(2)	(3)	(4)	(5)	(6)
	Source income agriculture	Source income fishing	Source income industry	Pollution from soil/water	Number of diarrhea	Number of leptospirosis/cholera
Treat	0.143***	-0.022	-0.047	-0.135***	-0.499	-0.213
	(0.046)	(0.020)	(0.030)	(0.051)	(0.359)	(0.150)
Post	0.000	0.000	0.000	0.000	0.000	0.000
	(.)	(.)	(.)	(.)	(.)	(.)
Treat * Post	0.001	-0.000	0.017	0.200**	0.301*	0.059**
	(0.050)	(0.017)	(0.049)	(0.085)	(0.173)	(0.030)
Number of industry center	0.000	-0.001	-0.000	-0.008**	0.074**	-0.006
	(0.002)	(0.001)	(0.001)	(0.004)	(0.038)	(0.009)
Constant	0.469***	0.222***	0.087***	0.213***	0.472	1.175***
	(0.036)	(0.016)	(0.017)	(0.027)	(0.311)	(0.129)
Observations	4889	4889	4889	4889	4889	4889
R2	0.88	0.96	0.51	0.67	0.50	0.97
Mean Dep Variable	0.90	0.01	0.03	0.03	0.30	1.03

Notes: *P < 0.10; **P < 0.05; ***P < 0.01. The dependent variables are the natural logarithms of annual agricultural production from 2010 to 2022 and monthly fishery variables in 2018 and 2021. Samples used to generate the reported estimates are restricted to villages within 50 km of the nearest nickel mine site. All specifications include climate controls, village fixed effects, mine-site fixed effects, year fixed effects, and province-by-year fixed effects. Standard errors are clustered at the grid level.